Letters

Transient Thermal Characterization and Assessment of Power Module With Encapsulated Phase Change Material Toward Overload Capability

Yuxi Liang, Peng Sun, *Student Member, IEEE*, Yiming Gong, Senhao Liang, Jiakun Gong, Huayang Zheng, Zheng Zeng, *Member, IEEE*, and Li Ran, *Fellow, IEEE*

***Abstract*—To mitigate transient thermal surge induced by the overload conditions in diverse applications, phase change materials (PCMs) have been proposed as an effective thermal management solution, offering enhanced heat capacity to maintain the power module within the safe operating area. However, PCM-integrated power modules face significant challenges, including excessive cost, process complexity, and increased steady-state thermal resistance. Besides, the absence of thermal models, insufficient understanding of thermal interactive mechanisms, and the lack of standardized evaluation criteria constrain the advanced thermal design for the packaging and practical application of PCM-based modules. To fill these gaps, this letter proposes a cost-effective and process-compatible overload-enhanced power module by the in-situ replacement of silicone gel with paraffin wax. Considering the impact of phase change transient on the junction temperature during the overload conditions, an improved thermal model is created by introducing the temperature-dependent heat capacity. Moreover, the thermal impedance of paraffin wax-coated power modules is comprehensively investigated by the finite element simulations. To quantify the overload capability, evaluation metrics comprising the optimal overload duration and the overall overload capability are proposed. Finally, power modules encapsulated with paraffin wax are fabricated, experimentally characterized, and evaluated. It is demonstrated that the proposed design provides an additional phase-change thermal impedance of 0.006 K/W with the steady-state thermal resistance maintained at 0.12 K/W compared to its silicone gel-encapsulated counterparts, thus offering a novel packaging approach and a thermal impedance-oriented evaluation criterion for power modules with high overload capability.**

***Index Terms*—Modeling and characterization, overload capability, phase change material (PCM), power module, thermal impedance.**

Received 6 May 2025; revised 10 June 2025 and 5 July 2025; accepted 29 July 2025. Date of publication 1 August 2025; date of current version 8 September 2025. This work was supported in part by the National Natural Science Foundation of China under Grant 52177169 and in part by the Chongqing Research Program of Basic Research and Frontier Technology under Grant CSTB2024NSCQ-JQX0016. *(Corresponding author: Zheng Zeng.)*

Yuxi Liang, Peng Sun, Yiming Gong, Senhao Liang, Jiakun Gong, Huayang Zheng, and Zheng Zeng are with the State Key Laboratory of Power Transmission Equipment Technology, School of Electrical Engineering, Chongqing University, Chongqing 400044, China (e-mail: yuxiliang@cqu.edu.cn; sunpeng_96@cqu.edu.cn; gongyiming@cqu.edu.cn; liangsenhao@cqu.edu.cn; gonjiakun@cqu.edu.cn; huayang_z@cqu.edu.cn; zengerzheng@cqu.edu.cn).

Li Ran is with the State Key Laboratory of Power Transmission Equipment Technology, Chongqing University, Chongqing 400044, China, and also with the School of Engineering, University of Warwick, CV4 7AL Coventry, U.K. (e-mail: l.ran@warwick.ac.uk).

Color versions of one or more figures in this article are available at https://doi.org/10.1109/TPEL.2025.3594604.

Digital Object Identifier 10.1109/TPEL.2025.3594604

I. Introduction

DUE to the load fluctuation, short-circuit faults, and rotor stalling in the field of renewable energy, electric vehicle, and aerospace, power converters frequently suffer from overload conditions, leading to a rapid junction temperature surge, which may push the power modules beyond the safe operating area, thus causing the potential device failure [1]. Therefore, enhancing the overload capability of power modules is critical for the reliable operation of power converters under various application scenarios. Phase change materials (PCMs) offer a promising thermal management solution by providing additional thermal capacitance during the overload operation, absorbing the excess heat flux without interfering with the normal operation [2]. However, integrating PCMs into power modules remains challenging owing to the reliability concerns, process complexity, and sealing demands, limiting their widespread adoption.

Some researchers have investigated the thermal behavior of power modules with overload capability. Regarding the packaging structure, PCMs are integrated into different layers of power modules, including the bottom and top chips [3], copper lead frame [4], thermal interface materials [5], and cooling fluids [6]. Thanks to the contributions mentioned before, the power modules support the overload capabilities. However, the modified packaging structure challenges the mass-production compatibility. Concerning the thermal characterization, the thermal buffering effect on the junction temperature of PCM-integrated modules has been thoroughly analyzed under varying overload ratios [7], durations [8], and cooling arrangements [9]. Nevertheless, the thermal impedance and model of PCM-integrated modules are often overlooked, leaving the interaction mechanisms of packaging layers unclear. Furthermore, the intrinsic thermal characterization requires excluding the influences of ambient temperature and power losses. Therefore, the thermal impedance analysis for PCM-integrated power modules remains an unexplored research gap.

To bridge these gaps, this letter proposes a cost-effective, process-compatible, and overload-capable power module by the in-situ replacement of silicone gel with paraffin wax, and the transient thermal principles of the proposed modules are elucidated via both thermal model and multiphysics tool. Besides, a thermal impedance-oriented evaluation criterion for the overload capability of power modules is developed. The rest

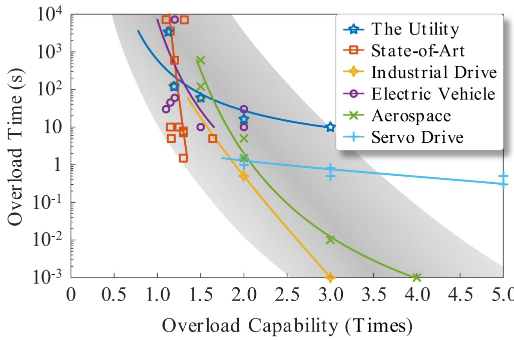

Fig. 1. Overload capability requirement and state-of-the-art of power module.

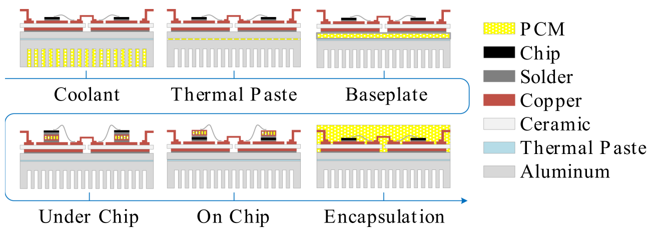

Fig. 2. Schematic power modules with PCM integrated at different layers.

of this letter is organized as follows. The pursuits for high overload capability in diverse application fields and the demands on PCM-integrated power modules are emphasized in Section II. In Section III, the thermal impedance model of the proposed power module is created and analyzed. In Section IV, the heat transfer mechanism and performance evaluation methods are presented by simulation tools. Comprehensive experiments and analyses are carried out in Section V. Some conclusions are summarized in Section VI.

II. Thermal Characterization Obstacle for Customized Design of PCM-Integrated Power Module

Overload capability is the widely emerging pursuit of converters for renewable energy and transportation electrification implementations, as illustrated in Fig. 1. For example, to handle the grid faults, grid-tied inverters are desired to enable three times of overload capability for 10 s. However, the overload capability of the existing power modules falls below the industry standards, particularly for grid-interfaced inverters and industrial control converters. As a result, to address the overload issues across diverse application conditions, customized power modules with high-overload capability are urgently needed.

To enhance the overload capability, integrating PCMs into different layers of power modules is emerging as the predominant solution, as shown in Fig. 2. However, the structural modifications to conventional packaging may lead to increased manufacturing complexity, compromised reliability, and extended thermal paths, which may degrade the steady-state heat dissipation performance. Thus, in-situ replacement of silicone gel with PCMs is proposed in this letter to offer a promising alternative due to its near-junction cooling design and process compatibility. Thanks to the stability, nontoxicity, lightweight features, and adjustable melting point, paraffin wax is a prospective candidate encapsulation of power modules. Besides, considering the sealing issue, adding an additional layer of epoxy resin on top of the PCM is a cost-effective solution for the housing of power modules.

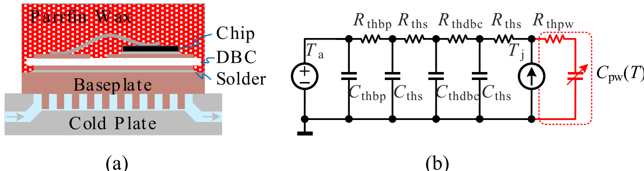

Fig. 3. Thermal impedance of PCM power module with encapsulated paraffin wax. (a) Stacked packaging structure. (b) Refined Cauer thermal model.

III. Thermal Impedance Modeling of PCM Integrated Power Modules

To characterize the thermal behavior of the proposed PCM-coated power module, it is essential to establish the thermal impedance model. The investigated power module is composed of a multilayer stack of heterogeneous materials, as illustrated in Fig. 3(a). The bottom-side thermal path comprises six stacked layers, including solder, copper–ceramic–copper direct bonded copper (DBC), solder, and baseplate, while the top-side path consists of paraffin wax.

To model the temperature plateau phenomenon caused by the latent heat effects, the temperature-dependent heat capacitance is introduced, whose relationship is restricted by the Dirac delta function, which exhibits a significant pulse within the phase transition temperature range [10]. Consequently, to simplify analysis, the heat capacitance of the paraffin wax $C_{\text{pw}}(T)$ in the thermal model can be approximately characterized as a piecewise function as

$$C_{\text{pw}}(T) = \begin{cases} C_{\text{ps}} & T \leq T_{\text{m}} \\ C_{\text{ps}} + L_{\text{m}}/\Delta T & T_{\text{m}} < T \leq \Delta T \\ C_{\text{pl}} & T \geq T_{\text{m}} + \Delta T \end{cases} \tag{1}$$

where C_{ps}, C_{pl}, L_{m}, T_{m}, and ΔT represent the specific heat capacity of the solid phase, the liquid phase, the latent heat, the phase change temperature, and the range of the transition temperature, respectively. In addition, the heat flux generated by the chip needs to be initially injected into the PCM before progressively accumulating. Therefore, the thermal resistance of PCM should be placed ahead of the thermal capacitance in the Cauer model, as shown in Fig. 3(b), where R_{thbp}, C_{thbp}, R_{ths}, C_{ths}, R_{thdbc}, C_{thdbc}, R_{thpw}, and C_{thpw} represent the thermal resistance and thermal capacitance of baseplate, solder, DBC, and paraffin wax, respectively. Noted that R_{thpw} consists of the contact thermal resistance between the encapsulant and the heat source, as well as the intrinsic thermal resistance of the paraffin wax. Besides, due to the similar thermal resistance of silicone gel and paraffin wax, the proposed module maintains the same thermal resistance, while its thermal response is significantly modified by the large transient thermal capacitance.

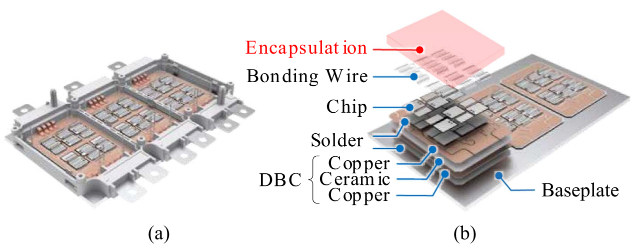

Fig. 4. Configuration of the studied power module. (a) Overall and (b) teardown views.

TABLE I
MATERIAL PROPERTIES USED IN MULTIPHYSICS MODEL

Properties	Cu	Solder	Al_2O_3	Si
Thermal Conductivity [W/(m·K)]	400	48	35	130
Specific Heat Capacity [J/(kg·K)]	385	150	730	700
Density (kg/m^3)	8960	9000	3965	2329

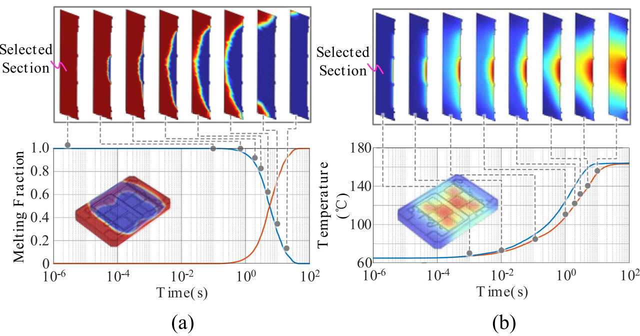

Fig. 5. Phase transition behavior of the proposed power module with encapsulated PCM. (a) Liquid phase fraction and (b) temperature distribution.

IV. SIMULATION VALIDATIONS AND ANALYSES

A. Studied Cases of PCM-Integrated Power Modules

To obtain the thermal impedance of the proposed power module, the FS820R08A6P2 IGBT module from Infineon is utilized as a baseline, as illustrated in Fig. 4. The silicone gel encapsulation material of the power module is replaced by paraffin wax. The properties of each layer material are listed in Table I.

The multiphysics approach is employed to analyze the transient thermal behavior of the proposed power module. As illustrated in Fig. 5(a), the paraffin wax begins to melt from the central chip at approximately 10 ms and gradually diffuses outward. By around 10 s, the paraffin wax fully transitions from the solid to the liquid phase. Besides, the temperature diffusion aligns with the melting progression of the paraffin wax, as shown in Fig. 5(b). Noted that the heat flux is initially transferred to the paraffin wax and then gradually accumulates on account of the latent heat effect, which is consistent with the theoretical analysis presented in Section III.

Besides, to evaluate the impact of PCM encapsulant on the uniformity of temperature distribution in the module, the standard variation of the average junction temperature among the three paralleled chips is summarized in Table II. It is observed

TABLE II
COMPARISON OF STANDARD VARIATION AMONG PARALLELED CHIPS IN POWER MODULES WITH DIFFERENT ENCAPSULANTS

Time (s)	Silicone Gel (°C)	Paraffin Wax (°C)
0.1	0.21	0.17
1	2.75	2.37
10	3.87	3.75
100	3.85	4.00

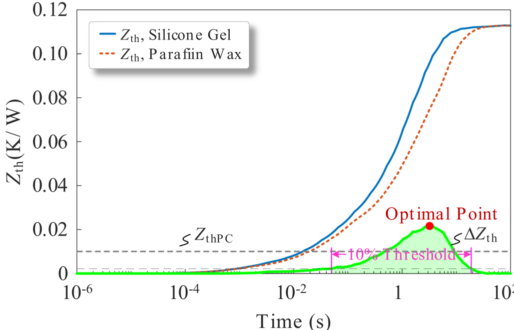

Fig. 6. Comparison of the thermal impedances for power modules with different encapsulation materials.

that the use of PCM as encapsulant does not lead to significant improvement in temperature uniformity throughout the phase transition period due to the small thermal spreading angle of PCMs [11], [12].

Moreover, the thermal impedance of modules encapsulated with the silicone gel and the paraffin wax can be derived, denoted as Z_{thjfs} and Z_{thjfp}, respectively, as shown in Fig. 6.

It is evident that Z_{thjfp} exhibits a significant dip, with a transient thermal impedance difference ΔZ_{th} around 13.4%. The peak of the ΔZ_{th} curve reflects the optimal overload duration, with a 24 °C junction temperature reduction at 3.6 s / three times the overload capability for the proposed module. Besides, the 10% threshold of ΔZ_{th} signifies the effective range of overload duration, spanning from 10 ms to 22 s for the module with paraffin wax encapsulation. Furthermore, the integral average of ΔZ_{th} within the 10% threshold, described as phase-change transient thermal impedance Z_{thPC}, represents the overall overload capability of the PCM-integrated power module. For instance, the Z_{thPC} of the silicone gel encapsulated modules equals 0, while the Z_{thPC} of the PCM-based modules is 0.01 K/W. Therefore, Z_{thPC} is a critical and unique indicator concerning the performance assessment and the degradation analysis for PCM modules. Furthermore, the proposed thermal assessment method is suitable for a more reliable power module with enhanced top-side interconnections, including copper wires, copper ribbons, and copper clips.

B. Principles of Encapsulated PCM on Thermal Impedance

To reveal the influence principles of the PCM properties on the thermal impedance for the PCM-coated power module in Fig. 4, a series of parameter sweep simulations are conducted, and the results are shown in Fig. 7.

To quantitatively evaluate the impact of material properties on the thermal impedance curves, a parameter sensitivity δ is

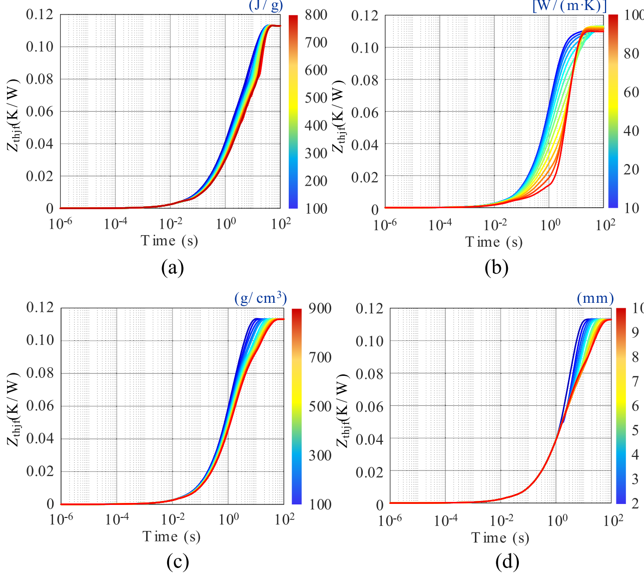

Fig. 7. Thermal impedance of PCM-coated power module influenced by material properties of (a) latent heat, (b) thermal conductivity, (c) mass density, and (d) height.

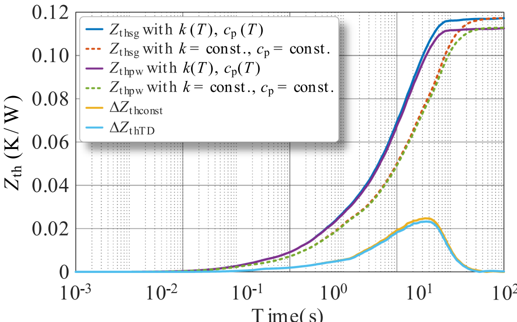

Fig. 8. Comparison of the thermal impedances for power modules with different encapsulations by considering material properties as temperature-dependent $k\,(T)$, $c_{\mathrm{p}}\,(T)$, and constant k, c_{p}.

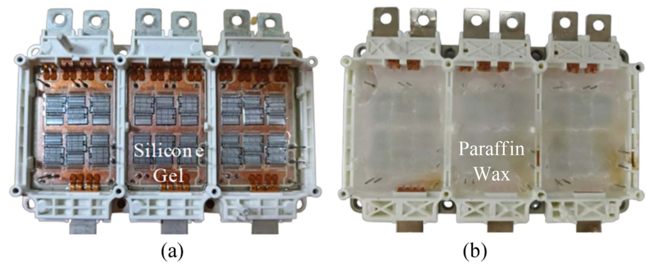

Fig. 9. Fabricated power modules encapsulated with (a) silicone gel and (b) paraffin wax.

TABLE III
SENSITIVITY OF MATERIAL PROPERTIES ON THERMAL IMPEDANCE OF PCM POWER MODULE

Parameter	Sensitivity δ(%)
Latent Heat	2.76
Thermal Conductivity	**7.16**
Mass Density	2.98
Height	2.88

defined as

$$\delta = \frac{\|Z_{\mathrm{thjf,max}} - Z_{\mathrm{thjf,min}}\|}{|x_{\max} - x_{\min}|} \times 100\% \tag{2}$$

where $x_{\max}$, $x_{\min}$, Z_{thjfmax}, and Z_{thjfmin} represent the maximum and minimum values of a specific material parameter and the corresponding thermal impedance curves, respectively. The notation $\|\cdot\|$ denotes the norm of the vector, which is used to quantify the distance between the thermal impedance curves. Subsequently, the sensitivity of different parameters, including the latent heat, thermal conductivity, mass density, and thickness of the PCM, is calculated and listed in Table III.

It is noted that the thermal conductivity of the PCM has the most significant impact on transient thermal response, which decides the heat transfer efficiency, as shown in Fig. 7(b), while the effect of latent heat is relatively minor owing to the limited thermal conductivity, as illustrated in Fig. 7(a). Besides, since the increased density of PCMs means the rise of per unit volume of PCM masses, an obvious suppression effect of the transient thermal effect throughout the entire phase change process is observed. However, enlarging the thickness of PCM can only improve the thermal buffering performance after 1 s, owing to the extended thermal path, as shown in Fig. 7(c) and (d). Therefore, the transient thermal performance of the PCM-integrated power modules can be improved through strategies including modifying material properties, as well as increasing the amount of PCMs.

C. Principle of Nonlinear Temperature Dependence of Materials on Thermal Impedance

Due to the significant nonlinear temperature dependence of thermal conductivity k and specific heat capacity c_{p} in stacked heterogeneous material layers, the corresponding influences on the ΔZ_{th} is necessary to be investigated. As illustrated in Fig. 8, two sets of thermal impedance curves of power modules with different encapsulation are obtained through FEA simulations, with c_{p} and k modeled as either temperature-dependent or constant parameters. It is noted that the steady-state thermal resistance of the power modules increases as $k\,(T)$ decreases with rising temperature. However, the influence of $c_{\mathrm{p}}\,(T)$ in non-PCMs on transient thermal impedance is negligible [13]. In contrast, $c_{\mathrm{p}}\,(T)$ in PCMs can be regarded as a special case of temperature-dependent material behavior, which significantly affects the transient thermal impedance and leads to a concave Z_{th} curve. Furthermore, the ΔZ_{th} is defined as the difference term of the two Z_{th}, effectively eliminating the impact of steady-state thermal resistance change caused by temperature dependence. The calculated ΔZ_{th} values with and without considering temperature dependence are 0.0127 K/W and 0.0132 K/W, respectively, with a relative error of approximately 4%. These results indicate that ΔZ_{th} primarily reflects the transient thermal impedance between power modules with different encapsulation materials, thereby verifying the feasibility and effectiveness of the proposed concept of Z_{thPC}.

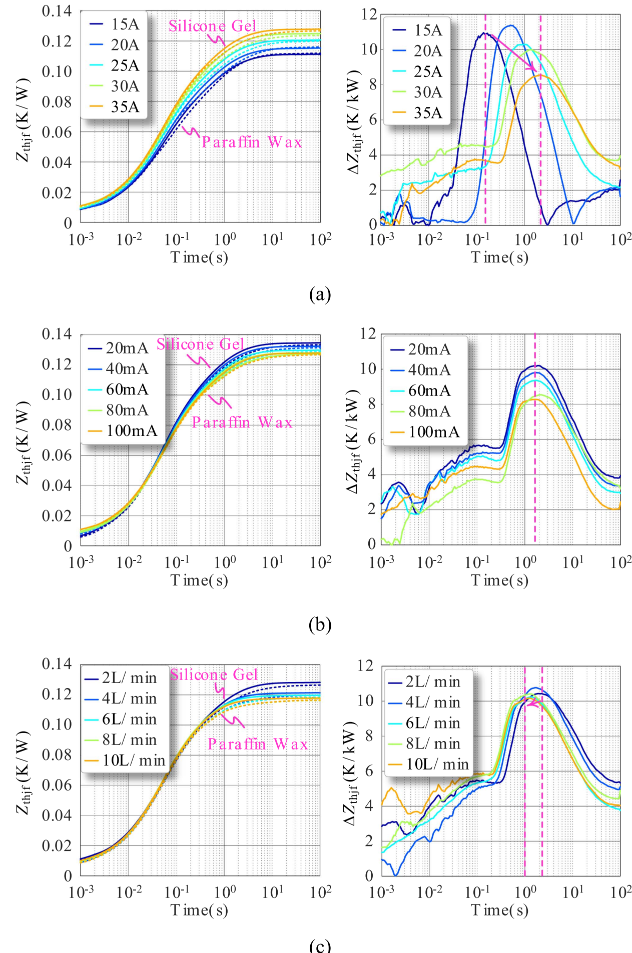

Fig. 10. Measured junction-fluid thermal impedance of power modules with different encapsulation materials influenced by (a) heating current, (b) sensing current, and (c) flow rate.

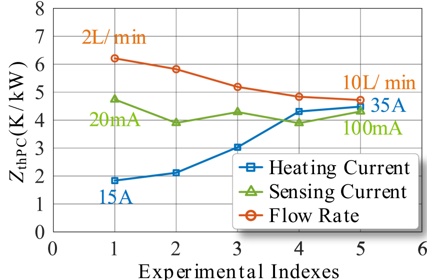

Fig. 11. Comparison of integral for differential thermal impedance under different experimental variables.

V. Experimental Validations

A. Transient Thermal Impedance Measurement

To confirm the overload capability of the proposed power module and the feasibility of the corresponding evaluation criterion, the prototypes of power modules encapsulated with silicone gel and paraffin wax were fabricated, as displayed in Fig. 9. Noted that the paraffin wax-coated power module is prepared by encapsulating melted paraffin wax after removing the original silicone gel using a gel breaker. Furthermore, the JESD51-14 standard is employed to extract the thermal impedance of each power module, with the collector–emitter voltage V_{CE} selected as the temperature-sensitive parameter [14].

The measured Z_{thjf} of power modules encapsulated in silicone gel/paraffin wax under different conditions is shown in Fig. 10. Due to the raised fluid temperature caused by the increased heating current, the elevated steady-state single-chip thermal resistance R_{thjf} is observed, reaching 0.128 K/W under a current of 35 A, as displayed in Fig. 10(a). Meanwhile, owing to the heat accumulation, more mass of PCM melt, thus intensifying the phase change effect, causes the peak of ΔZ_{thjf} shift from 140 ms to 2.1 s. As presented in Fig. 10(b), on account of the enhanced voltage drop across the contact resistance, a smaller sense current resulted in the overestimation of R_{thjf} around 5.5%, while since the actual phase change behavior remained unchanged, the peak of ΔZ_{thjf} remained stable at 1.5 s. As described in Fig. 10(c), by increasing the coolant flow rate, the measured R_{thjf} falls inversely from 0.128 K/W at 2 L/min to 0.116 K/W at 10 L/min, benefiting from the improved convective heat transfer coefficient. Nevertheless, due to the divert of heat flux to the bottom thermal path of the power modules, the conducted heat to the PCM layer was reduced, thereby moving the peak of ΔZ_{thjf} earlier from 2.2s to 0.9 s.

Furthermore, the Z_{thPC} under different test conditions is indicated in Fig. 11. It reveals that higher heating currents enhance the overload capability because of the increased PCM involvement. Besides, when the heating current reaches 30 and 35A, due to the full melting of the paraffin wax above the chips, the Z_{thPC} nearly stabilizes, thus indicating the maximum utilization efficiency of the latent heat from the PCM encapsulant. In contrast, the elevated coolant flow rates reduce the transient thermal contribution from the PCM layer, slightly degrading the overall overload performance. Notably, the sensing current has negligible influence on the integral value, confirming the reliability of the thermal impedance-oriented evaluation method for PCM-based power modules.

B. Converter-Level Operation Validation

As illustrated in Fig. 12, to verify the feasibility and effectiveness of the power module with encapsulated PCM, a front-to-front structure is selected, composed of two modules forming an H-bridge, where the silicone gel-encapsulated module is used as the auxiliary module, and the power module integrated with either paraffin wax or silicone gel is designated as the device under test. Besides, to achieve online junction temperature monitoring, the thermocouples are affixed to the chip surface by using the high-temperature-resistant adhesive before the encapsulation process.

To demonstrate the transient thermal storage capacity of the PCM encapsulant, the temperature curves of the two types of modules under three times the overload condition are captured. As described in Fig. 13(a), compared with the conventional power module, the junction temperature rise rate is effectively suppressed, resulting in an approximate 16 °C reduction in junction temperature after 5 s of overload. Besides, as illustrated

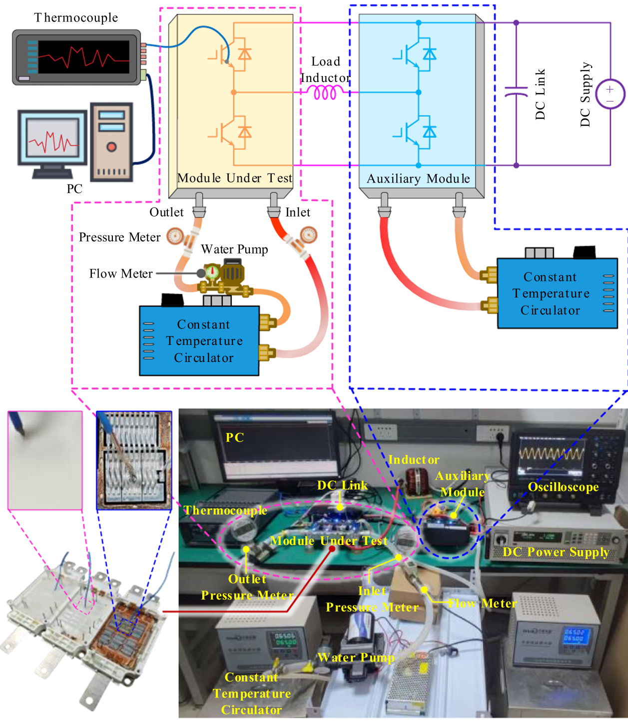

Fig. 12. Configuration of experimental setup for converter-level validation.

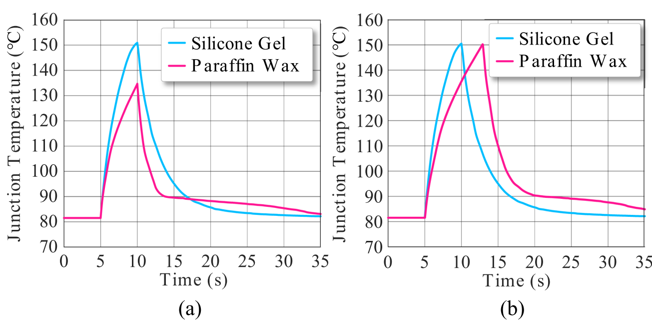

Fig. 13. Comparison of junction temperature under the three times overload condition. (a) Identical duration. (b) Identical peak temperature.

in Fig. 13(b), the overload duration of the proposed power module has been effectively extended from 5 to around 8 s, validating the enhanced overload capability of the PCM-integrated power module.

VI. Conclusion

The PCM is promised to fertilize the power module with overload capability for the utility, vehicle, and aerospace applications. However, the modified packaging structure poses challenges to the widespread adoption of the PCM-integrated power modules. Furthermore, the missing transient thermal characterization method and evaluation criteria lock the design and packaging of the power module with PCM integration. This letter proposed an overload-capable power module by the in-situ replacement of silicone gel with paraffin wax without significant structural changes. The thermal model is created to understand the transient thermal principles of the proposed power module with PCM encapsulated. To quantify the overload capability of the PCM module, the phase-change thermal impedance is defined, calculated by the integrity of the ΔZ_{th} determined by the Z_{th} curves of power modules with silicone gel and paraffin wax encapsulation. Detailed simulation and experimental results ensure the overload capability of the proposed module and the feasibility of the developed evaluation criterion. It is found that the proposed module offered an additional phase-change transient thermal impedance of 0.006 K/W with the steady-state thermal impedance maintained at 0.12 K/W compared with the silicone gel-encapsulated counterparts. Furthermore, the converter-level experiments show that the proposed module exhibits an approximate 16 °C reduction in junction temperature after 5 s of overload, enabling an extended overload duration of 3 s, demonstrating the competitive overload capability of the proposed module. Critical insights for novel packaging approaches and thermal performance evaluation methodologies have been provided in this letter for the next-generation power module with enhanced overload capability.

References

[1] S. Bhadoria et al., "Enablers for overcurrent capability of silicon-carbide-based power converters: An overview," *IEEE Trans. Power Electron.*, vol. 38, no. 3, pp. 3569–3589, Mar. 2023.

[2] W. Shao et al., "A power module for grid inverter with in-built short-circuit fault current capability," *IEEE Trans. Power Electron.*, vol. 35, no. 10, pp. 10567–10579, Oct. 2020.

[3] S. Bhadoria, S. G S, and H.-P. Nee, "Comparison of top and bottom cooling for short duration of over-currents for SiC devices: An analysis of the quantity and location of heat-absorbing materials," *IEEE Open J. Power Electron.*, vol. 5, pp. 765–778, 2024.

[4] R. Khazaka et al., "Analysis of power modules including phase change materials in the top interconnection of semiconductor devices," *Electron. Mater.*, vol. 5, no. 4, pp. 204–220, 2024.

[5] Semikron Danfoss, "Thermal interface materials," *Semikron Danfoss*, 2023. [Online]. Available: www.semikron-danfoss.com

[6] A. Stupar, U. Drofenik, and J. W. Kolar, "Optimization of phase change material heat sinks for low duty cycle high peak load power supplies," *IEEE Trans. Compon., Packag. Manuf. Technol.*, vol. 2, no. 1, pp. 102–115, Jan. 2012.

[7] H. Ren et al., "Thermal buffering effect of phase change material on press-pack IGBT during power pulse," in *Proc. IEEE Energy Convers. Congr. Expo.*, 2019, pp. 4937–4943.

[8] H. Jiang, J. Wei, X. Fang, H. Ren, W. Shao, and L. Ran, "A ΔT_j reduced power module with in-built phase change material for reliability enhancement," *IEEE Trans. Electron Devices*, vol. 68, no. 9, pp. 4557–4564, Sep. 2021.

[9] M. D. Rahman and X. Song, "A phase change material based silicon carbide power module packaging," in *Proc. IEEE 10th Int. Power Electron. Motion Control Conf.*, Chengdu, China, 2024, pp. 4916–4920.

[10] S. Moench and R. Dittrich, "Influence of natural convection and volume change on numerical simulation of phase change materials for latent heat storage," *Energies*, vol. 15, no. 8, 2022, Art. no. 2746.

[11] M. Xu et al., "Frequency-domain thermal coupling model of multi-chip power module," *IEEE Trans. Power Electron.*, vol. 38, no. 5, pp. 6522–6532, May 2023.

[12] Z. Zeng, K. Ou, L. Wang, and Y. Yu, "Reliability-oriented automated design of double-sided cooling power module: A thermo-mechanical-coordinated and multi-objective-oriented optimization methodology," *IEEE Trans. Device Mater. Rel.*, vol. 20, no. 3, pp. 584–595, Sep. 2020.

[13] S. Race, A. Philipp, M. Nagel, T. Ziemann, I. K. Badstuebner, and U. Grossner, "Circuit-based electrothermal modeling of SiC power modules with nonlinear thermal models," *IEEE Trans. Power Electron.*, vol. 37, no. 7, pp. 7965–7976, Jul. 2022.

[14] *Transient Dual Interface Test Method for the Measurement of the Thermal Resistance Junction-to-Case of Semiconductor Devices With Heat Flow Through a Single Path*, JEDEC Standard JESD 51-14, 2010.